Design of magnetic materials: the electronic structure of the ordered, doped Heusler compound $Co_2Cr_{1-x}Fe_xAl$

2005 J. Phys.: Condens. Matter 17 7237

(http://iopscience.iop.org/0953-8984/17/46/008)

INSTITUTE OF PHYSICS PUBLISHING JOURNAL OF PHYSICS: CONDENSED MATTER

J. Phys.: Condens. Matter **17** (2005) 7237–7252 doi:10.1088/0953-8984/17/46/008

Design of magnetic materials: the electronic structure of the ordered, doped Heusler compound $Co_2Cr_{1-x}Fe_xAl$

Gerhard H Fecher[1], Hem Chandra Kandpal[1], Sabine Wurmehl[1], Jonder Morais[2], Hong-Ji Lin[3], Hans-Joachim Elmers[4], Gerd Schönhense[4] and Claudia Felser[1]

[1] Institut für Anorganische Chemie und Analytische Chemie, Johannes Gutenberg-Universität, D-55099 Mainz, Germany
[2] Instituto de Fisica, Universidade Federal do Rio Grande do Sul, Porto Allegre, 91501-970 RS, Brazil
[3] National Synchrotron Radiation Research Centre—NSRRC, Hsinchu, 30076, Taiwan
[4] Institut für Physik, Johannes Gutenberg-Universität, D-55099 Mainz, Germany

E-mail: felser@uni-mainz.de

Received 8 August 2005, in final form 20 September 2005
Published 1 November 2005
Online at stacks.iop.org/JPhysCM/17/7237

Abstract

The doped Heusler compounds $Co_2Cr_{1-x}Fe_xAl$ with varying Cr to Fe ratio x were investigated experimentally and theoretically. The electronic structure of the ordered, doped Heusler compound $Co_2Cr_{1-x}Fe_xAl$ ($x = n/4, n = 0, 1, 2, 3, 4$) was calculated using band structure calculations of different types. The ordered compounds turned out to be ferromagnetic with the small Al magnetic moment aligned antiparallel to the 3d transition metal moments. All compounds show a gap around the Fermi energy in the minority bands. The pure compounds exhibit an indirect minority gap, whereas the ordered, doped compounds exhibit a direct gap. The magnetic circular dichroism in the x-ray absorption spectra was measured at the $L_{2,3}$ edges of Co, Fe, and Cr of the pure compounds and the $x = 0.4$ alloy in order to determine element-specific magnetic moments. Calculations and measurements show an increase of the magnetic moments with increasing iron content. The experimentally observed reduction of the magnetic moment of Cr can be explained by Co–Cr site disorder. The presence of the gap in the minority bands of Co_2CrAl can be attributed to the occurrence of pure Co_2 and mixed CrAl(001) planes in the $L2_1$ structure. It is retained in structures with different order of the CrAl planes but vanishes in the X structure with alternating CoCr and CoAl planes.

1. Introduction

Great scientific interest is aroused by materials with a complete spin polarization [1]. Such materials, being metals for spin up electrons and semiconductors (or insulators) for spin down electrons, are called half-metallic ferromagnets [2, 3] (HMF). Heusler compounds have been considered potential candidates for showing this property [2]. Theoretical calculations predicted an energy gap for minority electrons for the half-Heusler compound NiMnSb [2, 4] which, however, has been controversial [5–7]. Similarly, a HMF-like behaviour was found by Plogmann *et al* [8] for the Cobalt based Heusler alloy Co_2MnSn.

Heusler compounds belong to a group of ternary intermetallics with the stoichiometric composition X_2YZ ordered in an $L2_1$-type structure, many of which are ferromagnetic [9]. X and Y are transition metals and Z is usually a main group element. Y may also be replaced by a rare earth element. The cubic structure consists of four interpenetrating fcc lattices. The two fcc sublattices of the X atoms combine to a simple cubic sublattice. Remarkably, the prototype Cu_2MnAl is a ferromagnet even though none of its constituents is one [10]. The $L2_1$ structure of the Heusler compounds is shown in figure 1(a).

Ferromagnetic properties of various Heusler compounds have been investigated experimentally [9, 11–15] and theoretically [8, 16] (see [17, 18] for comprehensive review). The Co based Heusler compounds Co_2YZ are of particular interest because they show a comparatively high Curie temperature and varying magnetic moments ranging from 0.3 to 1.0 μ_B at the Co site depending on the constituents Y and Z (see [13, 19–21]).

The large variety of possible compositions of the Heusler compounds allows one to easily produce materials with predictable magnetic properties. The easiest way to compose new materials is by the exchange of one or more of the elements X, Y, and Z. This is indeed widely used in experiments and theory. See [16, 22–28] for examples on Co_2-containing Heusler compounds. However, the differences between the materials are rather rough. A better fine-tuning of magnetic properties may be obtained on substituting for one or another constituent only partially.

Such a way to design new materials is possible using a deliberate substitution of elements. Most often the main group element is kept fixed because the magnetic properties are mainly governed by the transition metal constituents. This leads to alloys of the type $X_{2-x}Y_{1+x}Z$, $(X_{1-x}X'_x)_2YZ$ or $X_2(Y_{1-x}Y'_x)Z$ ($x = 0, \ldots, 1$). The first type is still a ternary alloy whereas the second and third types result in quaternary alloys. Co based alloys of the first two types have been investigated by various groups [12, 19, 29–33].

This work focuses on quaternary alloys of the third type. The cobalt–aluminium based alloy of the $X_2(Y_{1-x}Y'_x)Z$ type with Y = Cr and Y′ = Fe is of particular interest as a base for materials design. This arises from the fact that the pure ($x = 0$ or 1) compounds exhibit the same lattice parameter within 0.1%. Therefore, partially replacing one element by another will lead to a material with the same lattice parameter but changed electronic and magnetic properties. Starting from the pure Cr-containing compound, the partial replacement by Fe may be seen as d electron doping.

$Co_2Cr_{0.6}Fe_{0.4}Al$ is of special interest because a relatively high magnetoresistance ratio of up to 30% was found in powder samples in a small magnetic field of 0.1 T [34, 35]. Thin films of the compound were successfully grown by several groups [36–39]. A magnetoresistance ratio of 26.5% [40] (at 5 K) and 19% [41] (at room temperature) was found for a tunnelling magnetoresistance (TMR) element of the same compound. Very recently, Marukame *et al* [42] reported a TMR ratio of 74% at 55 K for a $Co_2Cr_{0.6}Fe_{0.4}Al$–MgO–CoFe magnetic tunnel junction. A spin polarization of less than 49% was found for polycrystalline samples by means of Andreev reflections [43]. The observation of an incomplete spin polarization may not only

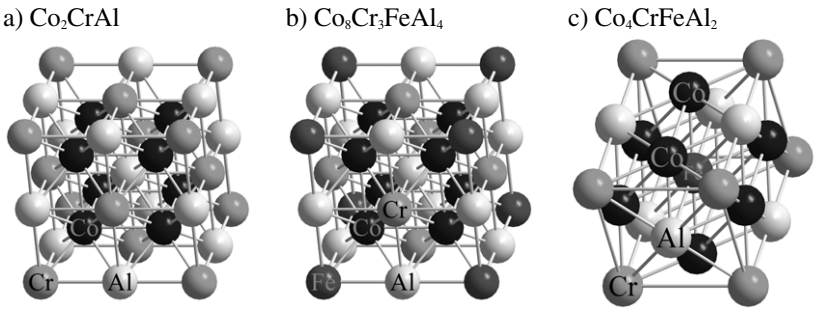

Figure 1. Structure of ordered $Co_2Cr_{1-x}Fe_xAl$: (a) $x = 0$, 1 ($L2_1$), (b) $x = 1/4$ (3/4 if exchanging Fe and Cr), and (c) $x = 1/2$ (see the text).

be caused by the model used to interpret the data [43, 44] but also by the properties of the sample. Clifford *et al* [45] reported recently a spin polarization of 81% at point contacts of $Co_2Cr_{0.6}Fe_{0.4}Al$.

For the purpose of the present study, doped Heusler alloys $Co_2Cr_{1-x}Fe_xAl$ were prepared by arc-melting under an argon atmosphere. The resulting specimens were dense polycrystalline ingots. Structural properties were measured using x-ray diffraction as a standard method. The cubic structure with a lattice constant of about 5.73 Å was confirmed for all samples. Flat discs (8 mm diameter by 1 mm thickness) were cut from the ingots. The discs were mechanically polished for spectroscopic experiments.

Field dependent magnetic properties were measured by SQUID magnetometry (temperature: 4–300 K) and by using the magneto-optical Kerr effect (MOKE) at room temperature. The remanent magnetization was less than 10% of the saturation magnetization, pointing to a soft magnetic material. Saturation was achieved for external fields above 0.2 T at 300 K. The Co_2CrAl samples in particular showed large differences in the total moment varying from 1 to 3 μ_B per formula unit. This depends mostly on the post-processing of the samples, like annealing followed either by quenching or slow cooling at different rates. In some cases, x-ray diffraction exhibited pronounced superstructures pointing to a tetragonal distortion of the unit cell. It should be noted that some types of disorder cannot be detected easily by means of x-ray powder diffraction as the scattering coefficients of Co and Cr are very similar. The same applies for neutron diffraction. Due to the nearly equal scattering length of Cr and Al, in particular, it is not possible to distinguish between ordered $L2_1$ and disordered B_2 structures. Therefore, we will use a detailed analysis of the magnetic properties to gain information about structural disorder of the samples. It should be noted that a mixing of Cr and Fe atoms in doped compounds will be hardly detectable by means of x-ray diffraction. This is a result of the very similar scattering coefficients of the constituting elements. An investigation of the x-ray magnetic circular dichroism (MCD) in soft x-ray absorption spectroscopy was performed at the *First Dragon* beamline of NSRRC (Hsinchu, Taiwan). The MCD measurements at the Cr, Fe, and Co $L_{2,3}$ absorption edges for $Co_2Cr_{1-x}Fe_xAl$ ($x = 0$, 0.4, and 1) were carried out in order to investigate element-specific magnetic properties and compare them with theoretical predictions. A Co_2CrAl sample free of superstructure but with a too low magnetic moment was selected for the MCD measurements in order to explain the large deviation from the expected value of 3 μ_B per formula unit. $Co_2Cr_{0.6}Fe_{0.4}Al$ was selected for the MCD measurements as this composition has shown the largest effect in measurements of the magnetoresistance.

More details about the experiment and the data analysis are reported in [35, 46].

The present work reports on calculations of the electronic and magnetic properties of ordered Heusler compounds of the type $X_2(Y_{(1-i/4)}Y'_{i/4})Z$. The calculated properties are

Table 1. Symmetry: space groups and Wyckoff positions of the constituents in ordered $Co_2Cr_{1-x}Fe_xAl$.

Compound		Co	Cr	Fe	Al
Co_2CrAl	$Fm\bar{3}m$	8c	4a	—	4b
$Co_8Cr_3FeAl_4$	$Pm\bar{3}m$	8g	1a	3c	1b, 3d
$Co_4CrFeAl_2$	$P4/mmm$	4i	1a	1d	1b, 1c
$Co_8CrFe_3Al_4$	$Pm\bar{3}m$	8g	3c	1a	1b, 3d
Co_2FeAl	$Fm\bar{3}m$	8c	—	4a	4b

compared to experimental values. Deviations from the $L2_1$ structure are discussed on the basis of ordered structures. Random alloys of the $X_2(Y_{(1-x)}Y'_x)Z$ type with non-rational values of x as well as random disorder (for examples see [47, 48]) will not be discussed here.

2. Calculational details

Self-consistent band structure calculations were carried out using the scalar-relativistic full potential linearized augmented plane wave method (FLAPW) provided by Blaha *et al* [49, 50] (Wien2k). The exchange–correlation functional was taken within the generalized gradient approximation (GGA) in the parametrization of Perdew *et al* [51]. For comparison, calculations were also performed using the linear muffin-tin orbital (LMTO) method provided by Savrasov [52] (LMTART 6.5) at different levels of sophistication from the simple atomic sphere approximation (LMTO-ASA) to the full potential plane wave representation (FP-LMTO-PLW). A $20 \times 20 \times 20$ k-point mesh was used for the integration in cubic systems.

The properties of the pure Cr- or Fe-containing compounds where calculated in $Fm\bar{3}m$ symmetry using the experimental lattice parameter ($a = 10.822a_{0B}$, $a_{0B} = 0.529\,177$ Å) as determined using x-ray powder diffraction. All muffin-tin radii were set for nearly touching spheres with $r_{MT} = 2.343a_{0B}$ in both full potential methods. The overlapping spheres where set with $r_{MT} = 2.664a_{0B}$ for the ASA calculations.

The full formula sum of the cubic cell is $X_8Y_4Z_4$, with X = Co, Y = Cr or Fe, and Z = Al and is reduced to $X_2YZ = Co_2YAl$. Exchanging Y and Z does indeed lead to identical structures. (See figure 1 and table 1 for the positions of the atoms.)

The calculation of mixed random alloys is not straightforward in the two (FLAPW and LMTO) calculational methods. However, replacing some Cr atoms of the $L2_1$ structure with Fe leads in certain cases to ordered structures that can be easily used for calculations. Ordered, mixed compounds may have the general formula sum $X_8(Y_{(1-x)}Y'_x)_4Z_4$ with Y = Cr and Y′ = Fe. These structures have integer occupation of Y and Y′ if $x = i/4$ with $i = 1, 2, 3$.

We start with the Cr atoms occupying the corners of the cube and the centre of the faces. The Al atoms are located at the middle of the cube edges (see figure 1(a)). Replacing the Cr atom at (0, 0, 0) by Fe leads to the structure with $x = 1/4$ (see figure 1(b)). The same structure may also be found if we start with Cr and Al exchanged and then replace the Cr atom at (1/2, 1/2, 1/2) with Fe. The symmetry of these structures is again cubic but reduced to $Pm\bar{3}m$. The only difference is that the base atoms are shifted.

Simply exchanging the Cr atoms of this structure for Fe leads to the structure with $x = 3/4$. The corresponding formula sums are $Co_8Cr_3FeAl_4$ and $Co_8CrFe_3Al_4$.

Again, we start with the Cr atoms occupying the corners and face centres of the cube. We replace two of the face Cr atoms, say those at (0, 1/2, 1/2), (1/2, 0, 1/2), and those at the opposite faces with Fe. The result is the structure with $x = 1/2$. This structure is initially cubic but can be reduced to tetragonal symmetry ($P4/mmm$) with the formula sum $Co_4CrFeAl_2$.

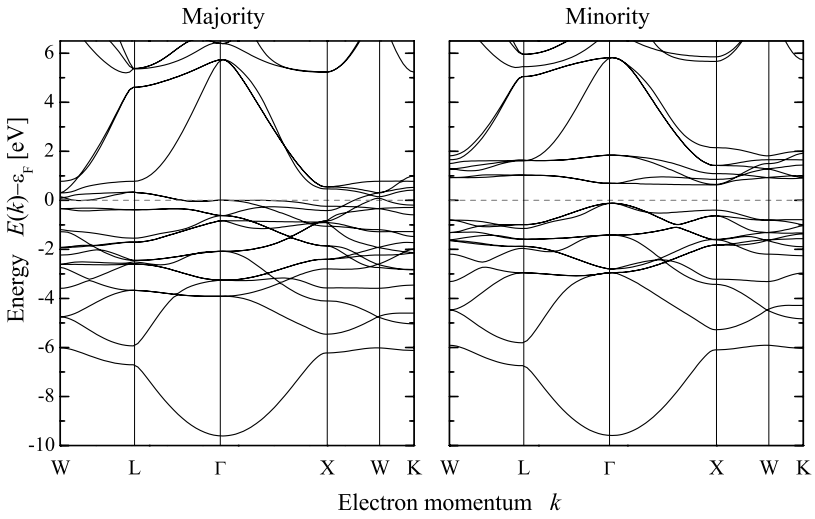

Figure 2. Band structure of Co_2CrAl.

The three different structures are illustrated in figure 1. The cell shown for $x = 1/2$ has a reduced, tetragonal symmetry. The z axis may be chosen such that the long c axis coincides with one of the cubic axes of the initial structure. The symmetry and the lattice sites of the structures are summarized in table 1.

Other ordered structures are found from larger elementary cells. The cubic cell doubled in all three directions has the overall formula sum $X_{64}(Y_{(1-x)}Y'_x)_{32}Z_{32}$. The special case with $x = 13/32$ is very close to the compound $Co_2Cr_{0.6}Fe_{0.4}Al$.

3. Results and discussion

The electronic structure of the pure and doped compounds will be discussed in the following. First, the band structure and the density of states of the ordered compounds are presented. This is followed by a more specific discussion of the magnetic properties on hand of measured and calculated magnetic moments.

A structural optimization was performed for Co_2CrAl and Co_2FeAl using FLAPW in order to validate using the experimental lattice parameter. The energy minima were found to appear at lattice parameters less than 0.5% smaller compared to the experimental values, for both materials. The calculated bulk moduli were 217 and 210 GPa for the Cr- and the Fe-containing compounds, respectively. None of the results discussed below changes significantly if one uses the optimized lattice parameter instead of the experimental one. In particular, the overall spin moments stay the same and the half-metallic behaviour of the ordered compounds is retained. Very small deviations appear for elemental resolved values. These are already sensitive to the setting of the r_{MT} and the number of k-points used for integration, as is well known. The differences between the observed and optimized structures are only small and we did not notice any deviation from Vegard's law for the mixed compounds.

3.1. Band structure and density of states

The self-consistent FLAPW band structure of Co_2CrAl is shown in figure 2. The energy scale is referenced to the Fermi energy (ϵ_F). The typical Heusler gap is located at about 6 eV binding energy. It separates the low lying s bands from bands of predominantly d character. These low

lying s bands emerge mainly from the main group element, here Al. This gap is very small in the Al-containing compounds. Much larger gaps are found for example in Sn-containing compounds like Co_2TiSn [53] and the half-Heusler NiMnSb [54].

From the spin resolved bands, it is seen that the majority bands cross or touch the Fermi energy (ϵ_F) in all directions of high symmetry. On the other hand, the minority bands exhibit a gap around ϵ_F, thus confirming a HMF character. For Co_2CrAl, the width of the gap is given by the energies of the highest occupied band at the Γ point and the lowest unoccupied band at the Γ or X point. The smaller value is found between Γ and X; thus it is an indirect gap. It should be noted that the direct gap at the Γ point is only 60 meV wider. Therefore, a small change in the parameters of the calculation may already change the character of the gap from indirect to direct. Indeed, some LMTO calculations resulted in a direct gap, most probably for just that reason.

We will restrict the following comparison of the doped compounds to cases with the Δ direction parallel to [001]. The Δ direction possesses in all cases C_{4v} symmetry. It has the advantage that the compound with $x = 1/2$ can be compared directly to the others although it is calculated for tetragonal symmetry where the corresponding Λ direction is between Γ and Z.

The Δ direction is perpendicular to the $Co_2(100)$ planes. As it will turn out later, just the Δ direction plays an important role for the understanding of the HMF character and magnetic properties of Heusler compounds. This role of the Δ direction was also pointed out by Öğüt and Rabe [55].

The band structures in the Δ direction of the pure ($x = 0, 1$) and the doped ($x = 1/2$) compounds are displayed in figure 3 for energies above the Heusler gap. In general, the doped compounds exhibit many more bands compared to the pure ones as a result of the lowered symmetry. Therefore, results are shown only for the mixed compound with equal Fe and Cr concentrations.

Compare the majority bands of the two pure compounds. At first sight, the Fermi energy is just higher in the Fe case compared to Cr, as expected from the larger number of d electrons. A closer look reveals more detailed differences. The indirect gap of the Δ direction (clearly seen for the Cr based compound) is not only shifted to below ϵ_F but nearly closes for the Fe based compound. This gap is also nearly closed in the majority bands of the mixed compound with $x = 1/2$ as well as those with $x = 1/4, 3/4$ (not shown here). This observation calls a rigid band model into question. In that case the bands would be simply filled with an increasing number of d electrons, leaving the shape of the bands unchanged.

More interesting is the behaviour of the minority bands, as they determine the HMF character of the compounds. Comparing again the Cr and the Fe based compounds, one finds that the energies of the states at Γ are nearly the same below ϵ_F. The shapes of the bands close to Γ are similar, too. The situation is different at X where the unoccupied states are shifted toward ϵ_F in Co_2FeAl compared to Co_2CrAl.

It is worth noting that the first unoccupied minority band of Co_2FeAl just touches ϵ_F at X. Therefore, any temperature above 0 K will immediately destroy the HMF gap due to the smearing of the DOS around ϵ_F (for additional temperature effects destroying the minority gap, see e.g. [56, 57]). Chioncel *et al* [58] reported for NiMnSb the occurrence of non-quasiparticle states just below the minority conduction band. A similar effect would immediately destroy the HMF character if it appeared in Co_2FeAl, too. The band structure of Co_2MnAl shows a behaviour at Γ, similar to that of Co_2FeAl. Here the minority bands even slightly cross the Fermi energy, as was found in calculations for comparison with the iso-electronic compound $Co_2Cr_{1/2}Fe_{1/2}Al$. Even if one accounts for small numerical deviations while calculating ϵ_F for the two compounds, they may not be good candidates for spin injection device use.

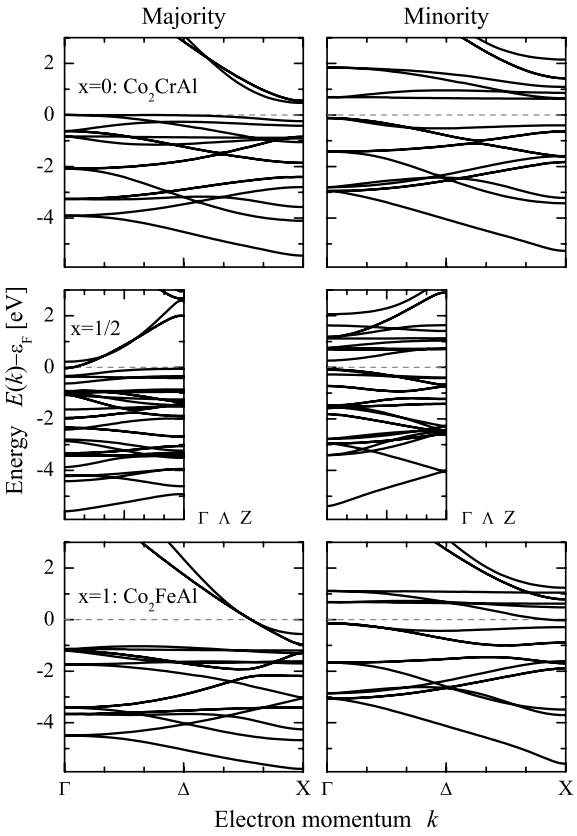

Figure 3. Δ, Λ bands of $Co_2Cr_{1-x}Fe_xAl$. (The high symmetry points are X for $x = 0, 1$ and Z for $x = 1/2$. Note that the absolute values of k are 1.1 $Å^{-1}$ at X for $x = 0, 1$ and only 0.55 $Å^{-1}$ at Z for $x = 1/2$.)

The mixed compounds are described by P lattices. Therefore, the Brillouin zone of these compounds is generally smaller compared to the F lattice. This results in a seeming back-folding of bands from the larger F Brillouin zone into a smaller one. This effect is accompanied with some additional splitting (removed degeneracies) at points of high symmetry.

Due to the manifold of bands in the mixed compounds, it is not easy to compare the results directly; therefore we concentrate on the width of the gap in the minority bands. This gap is mainly characterized by the bands in the Δ direction as found from the band structure for all directions of high symmetry (not shown here). More specifically, it is given by the energies at the Γ and X points of the Brillouin zone.

The width of the gap in the minority bands is shown in figure 4. The direct band gap at the Γ point becomes successively smaller with increasing iron content x and ranges from 750 meV at $x = 0$ to 110 meV at $x = 1$. The direct gap of Co_2FeAl is only 60 meV wider than the indirect one between Γ and X. The direct gap at Γ is much wider in Co_2FeAl; therefore this compound is characterized by the indirect gap only.

The character of the gap changes from indirect to direct going from pure to mixed compounds. This change of character of the gap in the Δ direction is a consequence of the smaller Brillouin zone in the mixed compounds that leads to a so-called back-folding of bands.

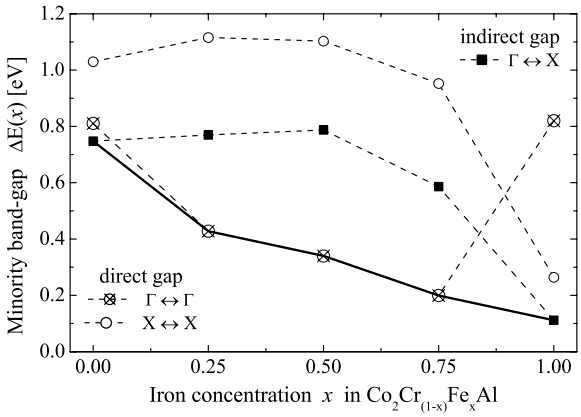

Figure 4. Minority band gap in $Co_2Cr_{1-x}Fe_xAl$. (Lines are drawn to guide the eye. The full line follows the limit for the HMF gap.)

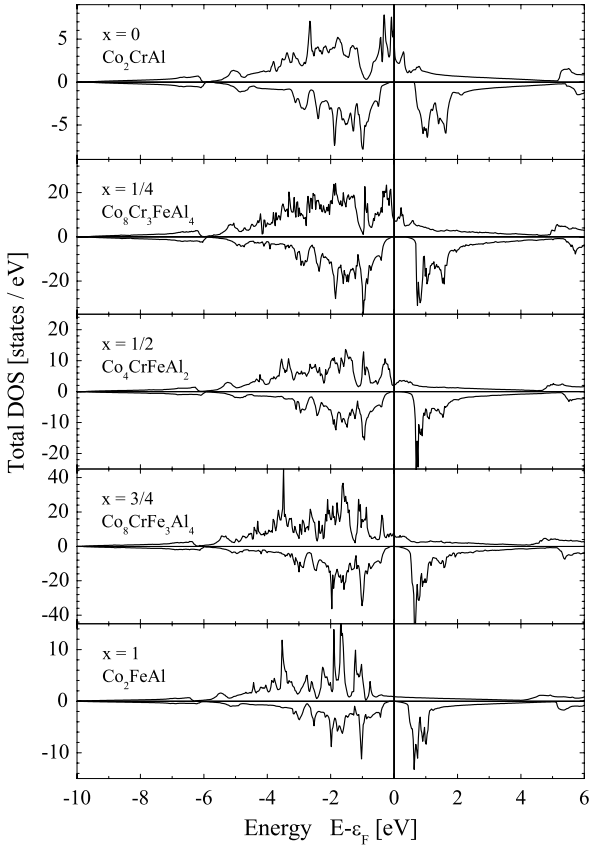

Figure 5. Total DOS of $Co_2Cr_{1-x}Fe_xAl$.

The total density of states (DOS) is shown in figure 5 for varying iron content x. The gap at the Fermi energy is clearly seen in the DOS of the minority states for all compounds. The total DOS shows also that the Heusler gap at about 6 eV binding energy is nearly closed.

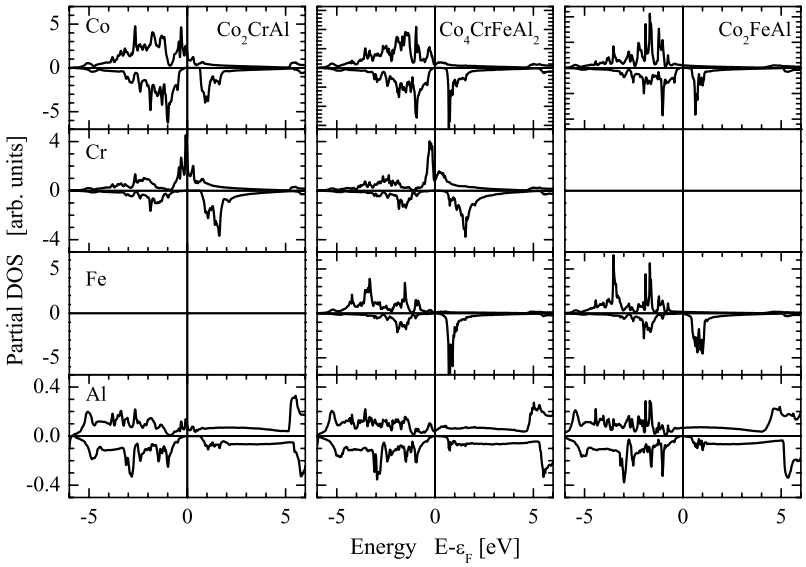

Figure 6. Partial DOS of $Co_2Cr_{1-x}Fe_xAl$ ($x = 0, 1/2, 1$).

The majority DOS at the Fermi energy decreases with increasing iron concentration x. The density of majority electrons at ϵ_F is a crucial point for spectroscopic methods investigating the spin polarization, like spin resolved photoemission. A complete spin polarization may be only detectable if there is a high majority density. The same may be true for spin injection systems where one is interested in a high efficiency.

It is also seen that the minority DOS seems to be much less affected by the Fe doping compared to the majority DOS. Mainly, the unoccupied part of the DOS above ϵ_F changes its shape, but not the occupied part.

In summary, it is found that doping of the compound with Fe changes mainly the occupied majority and the unoccupied minority DOS. Again it is seen that doping with iron results not just simply in a shift of the DOS as would be expected from a rigid band model. Majority and minority densities are altered in different ways.

More details of the change in the DOS and electronic structure can be extracted if we analyse the partial DOS (PDOS), that is the atom-type resolved density of states. The PDOS of the pure compounds is compared in figure 6 to the PDOS of the mixed compound with equal Cr and Fe contents ($x = 1/2$).

From figure 6, it is seen that the high majority DOS at the Fermi energy emerges from Cr. Both Co and Fe exhibit only a small majority PDOS at ϵ_F. Overall, the change of the majority DOS of $Co_2Cr_{1-x}Fe_xAl$ around ϵ_F can be clearly attributed to the increasing amount of iron with respect to chromium. The minimum in the minority DOS around ϵ_F is mainly restricted by the shape of the Co PDOS. This indicates that the HMF-like behaviour is mainly characterized by Co. The steep increase of the minority PDOS of Cr and Fe is mainly located in the unoccupied part above ϵ_F.

Doping with Fe not only changes the total DOS but also the PDOS of Co and Cr. In particular, the slight shift of the Cr PDOS to lower energies causes an additional decrease of majority states at ϵ_F. This shift increases with increasing Fe concentration, as was found from the PDOS for $x = 1/4$ and $3/4$ (not shown here). The slight energy shift of the PDOS will result in a small change of the local magnetic moments at the Co and Cr sites, as will be shown below.

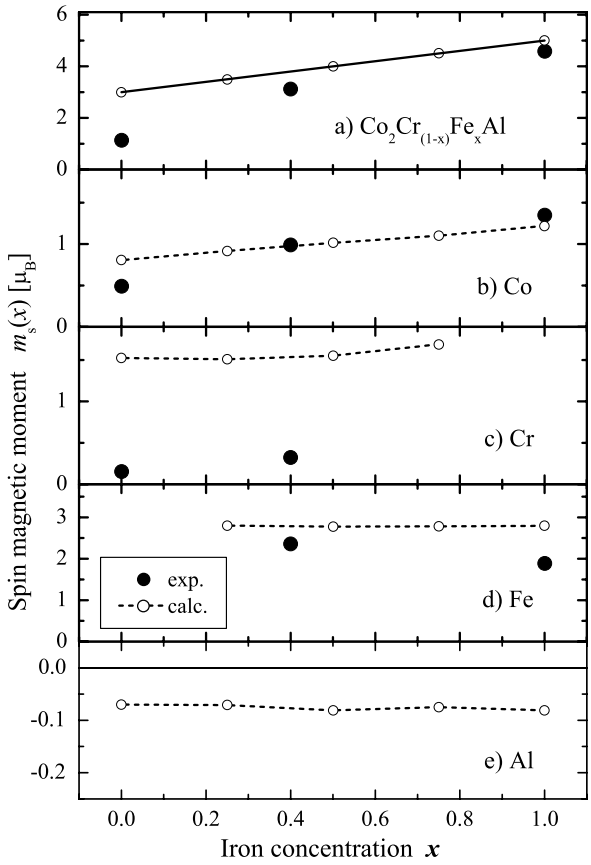

Figure 7. Magnetic moments of $Co_2Cr_{1-x}Fe_xAl$. The measured element-specific and total moments for ($x = 0$, 0.4, and 1) are compared to calculated values for ($x = 0$, 1/4, 1/2, 3/4, and 1). The full line in (a) corresponds to the *rule of thumb*; dashed lines in (b)–(e) are drawn through the calculated values to guide the eye.

The aluminium PDOS is rather unaffected by the Cr or Fe concentration. It exhibits only small energy shifts.

3.2. Magnetic moments

SQUID magnetometry and MCD were used to determine total and partial magnetic moments of $Co_2Cr_{1-x}Fe_xAl$. Details of these measurements are reported in [46]. The measured values are extrapolated to $T = 4$ K and calibrated using the total moments measured by the SQUID. Total and element-specific magnetic moments were extracted from the band structure calculations reported above. Figure 7 compares measured and calculated spin magnetic moments.

The calculated total spin magnetic moment follows a *rule of thumb* for Heusler compounds:

$$\mu_s = (N - 24)\mu_B. \tag{1}$$

N is the cumulated number of valence electrons (here: 4s, 3d for the transition metals Co, Cr, or Fe and 3s, 3p for the main group element Al). The value calculated from equation (1) is shown as a full line in figure 7(a).

Table 2. Magnetic moments in Co_2CrAl. Element-specific (per atom) and total spin magnetic moments (per formula unit) calculated by different methods.

	m_s (μ_B)		
Method	Co	Cr	Tot
LMTO-ASA	0.67	1.72	2.98
LMTO-ASA-GGA	0.70	1.63	2.98
FP-LMTO-PLW	0.73	1.61	3.01
FLAPW-GGA	0.81	1.52	3.00
KKR [28]	0.76	1.54	2.96

The calculated spin magnetic moments of Co and Fe are in agreement with the measured values. The measured, lower total value at small Fe concentration can be attributed clearly to a too low moment at the Cr sites.

The calculated spin moments of Co and Cr increase slightly with increasing Fe concentration, whereas the Fe moment stays nearly constant. This increase is explained by an energy shift of the partial densities of Co and Cr as discussed above.

The calculated Al spin moment is negative, independent of the Fe concentration. This points to an *antiferromagnetic* order of the Al moments with respect to the transition metal moments. However, the induced moments at the Al sites are only very small.

All values found here for the pure compounds are in the same order as those calculated by Galanakis *et al* [28] using the Korringa–Kohn–Rostoker (KKR) method.

It may be interesting to compare the magnetic moments of $Co_2Cr_{0.5}Fe_{0.5}Al$ with those of the nominally iso-electronic compound Co_2MnAl. Our calculations yielded 3.81 μ_B for the total spin moment per formula unit and 0.84 and 2.58 μ_B for the partial spin moments of Co and Mn, respectively. These values are similar to those found by other groups [23, 28] using KKR. The Co moment is larger in the mixed compound (1.01 μ_B) and the average $Cr_{0.5}Fe_{0.5}$ moment (2.24 μ_B) is smaller compared to that of Mn. It is interesting to note that the minority states were shifted at the Γ point to energies above ϵ_F, such that the HMF gap became closed in Co_2MnAl. A variation of the lattice parameters showed that this is not causing the differences between the two materials. The differences are caused by the different local potentials in those compounds.

Most evidently, the calculated magnetic moment of the Co_2CrAl compound does not agree with the measured one. The experimental value is only about 1.3 μ_B whereas theory predicts a value of about 3 μ_B per formula unit. The value found here is in rough agreement with the ground state magnetic moment of 1.55 μ_B per formula unit reported earlier by Buschow [59]. It was previously considered that it is mainly the Co atoms that carry the magnetic moment, whereas the contribution of Cr and Al atoms remains negligible [60]. This empirical assumption may describe the present element-specific measurements, revealing a moment of $\approx 2 \times 0.55$ μ_B for Co_2 but only ≈ 0.2 μ_B for Cr. However, it does not explain the physics behind that observation.

One may assume that the high magnetic moment of Cr is an artefact of a particular calculation scheme. Therefore, different calculation schemes were used to check the probable occurrence of such effects. The results are summarized in table 2. The results of Galanakis *et al* [28] derived from KKR calculations are shown for comparison. The partial and total magnetic moments calculated by Kellou *et al* [61] at a smaller lattice parameter (10.758 a_{0B}) are in the same range.

It is seen from table 2 that all values stay comparable within few %. Therefore, the deviation from the experiment cannot be attributed to the peculiarities of one or another

Table 3. Structural dependence of the magnetic moments in Co_2CrAl. Note: the sum of the magnetic moments of the two individual Co atoms and average values for Cr and Al are given to make different structures comparable. The total spin magnetic moment is given per formula unit.

		m_s (μ_B)			
	Structure	Co_2	Cr	Al	Total
$L2_1$	$Fm\bar{3}m$	1.42	1.63	−0.05	2.98
X	$F\bar{4}3m$	1.84	−0.83	−0.02	0.91
$cP16$	$Pm\bar{3}m$	1.69	1.48	−0.05	3.00
$tP4$	$P4/mmm$	1.82	1.47	−0.05	3.19
	Experiment	1.11	0.19	—	1.30

theoretical method. The Cr moment is about $(1.6 \pm 0.1)\mu_B$, rather independently of the method of calculation.

On the other hand, a reduction of the observed Cr moment may be caused by site disorder, such that some of the Cr atoms become antiferromagnetically ordered either among themselves or with respect to the Co atoms. The latter effect results in a ferrimagnetic order. A mixture of ordered and disordered crystallites will then result in a measured value being too small compared to the calculated moment. Such a disorder has to be realized with the same lattice parameter because x-ray diffraction did not show any superstructure in the samples investigated here.

To estimate the influence of disorder in the CrAl planes, the band structure was also calculated for the hypothetical $cP16$ ferrite structure ($Pm\bar{3}m$). In this structure, successive CrAl(001) planes are Cr or Al rich with 3:1 or 1:3 ratios, respectively. The calculated magnetic moments of Cr were about 1.5 μ_B. Lin and Freeman [62] used the tetragonal $tP4$ structure ($P4/mmm$) to simulate Y/Al disorder in Ni_2YAl (Y = Ti, V, etc). In this structure one has the series Co–Cr–Co–Al for the consecutive (001) planes instead of Co–(CrAl) (note that (100) and (001) planes are not equivalent in the tetragonal structure). Again, the calculated magnetic moment of Cr has about the same magnitude. A ground state with an antiferromagnetic or ferrimagnetic order of the Cr atoms could not be verified in either of the structures. Therefore, those structure can be excluded as possible candidates for providing an explanation of the reduction of the magnetic moment. This is in accordance with the x-ray diffraction data where no additional Bragg peaks were observed. Extra (001) Bragg peaks are expected for both structures, for example. However, it is worth noting that the compound still exhibited HMF character in the $cP16$ structure.

More promising are calculations for the X structure ($F\bar{4}3m$) [63]. (Note that the Pearson code of this structure is $cF16$ like for $L2_1$.) This structure was also considered among several phases with random antisite disorder by Feng *et al* [64] investigating the physical properties of Fe_2VAl. It is similar to the $C1_b$ half-Heusler phase but with the vacancies filled up in a different way compared to the $L2_1$ structure case. The X structure consists of successive CoCr and CoAl(001) planes.

The calculation reveals for the X structure an antiferromagnetic ordering of the Cr atoms with respect to Co and thus a reduced overall magnetic moment. The magnetic moments derived for the different structures are summarized in table 3.

The calculated, element-specific, and total magnetic moments are compared to experimental values in table 3. For Co the sum of the two atoms is given. The averages of the calculated values for Cr and Al are given for the structures with inequivalent atomic positions.

Table 4. Site symmetries in Co_2CrAl. PM—paramagnetic order; FM—ferromagnetic order with $B \parallel [001]$. The nearest distance d_{AB} between two atoms A and B is given in Å. The second and fourth lines for each structure give the Wyckoff positions of the atoms in the PM and FM state.

			Co	Cr	Al	d_{CoCo}	d_{CoCr}	d_{CrCr}	d_{CrAl}	Γ	Δ, (Λ) [0, 0, z]	X, (Z)
$L2_1$	PM	$Fm\bar{3}m$	T_d	O_h	O_h	2.86	2.48	4.05	2.86	O_h	C_{4v}	D_{4h}
$cF16$			8c	4a	4b							
	FM	$I4/m$	S_4	C_{4h}	C_{4h}					$D_{4h}(C_{4h})$	$C_{4v}(C_4)$	$D_{4h}(C_{4h})$
			4d	2a	2b							
X	PM	$F\bar{4}3m$	T_d	T_d	T_d	2.48	2.48	4.05	2.48	T_d	C_{2v}	D_{2d}
$cF16$			4a, 4c	4b	4d							
	FM	$I\bar{4}$	S_4	S_4	S_4					$D_{2d}(S_4)$	$C_{2v}(C_2)$	$D_{2d}(S_4)$
			2a, 2d	2b	2c							
$cP16$	PM	$Pm\bar{3}m$	C_{3v}	O_h, D_{4h}	D_{4h}, O_h	2.86	2.86	2.48	2.86	O_h	C_{4v}	D_{4h}
			8g	1a, 3d	3c, 1b							
	FM	$P4/m$	C_1	C_{4h}, C_{2h}, C_{2h}	C_{2h}, C_{2h}, C_{4h}					$D_{4h}(C_{4h})$	$C_{4v}(C_4)$	$D_{4h}(C_{4h})$
			8l	1a, 2e, 1b	1c, 2f, 1d							
$tP4$	PM	$P4/mmm$	C_{4v}	D_{4h}	D_{4h}	2.86	2.48	2.86	2.86	D_{4h}	C_{4v}	D_{4h}
			2h	1a	1b							
	FM	$P4/m$	C_4	C_{4h}	C_{4h}					$D_{4h}(C_{4h})$	$C_{4v}(C_4)$	$D_{4h}(C_{4h})$
			2h	1a	1b							

A more detailed analysis of the X structure shows not only an antiferromagnetic order of Cr but also an enhancement of the Co magnetic moments. Their values are 0.94 μ_B in CoAl and 0.76 μ_B in CoCr(001) planes. Evidently the shortest distance between two Co atoms is smaller in the X structure compared to the $L2_1$ structure (see table 4). The shortest Co–Cr and Cr–Cr distances stay the same in both structures.

The enhancement of the Co moments in all three non-$L2_1$ structures does not allow one to explain the experimentally observed moments directly because the measured value is already smaller as the calculated moment of the $L2_1$ structure. This is mainly a property of the particular sample investigated here. Other samples exhibited higher overall magnetic moments.

The gap in the minority band structure is closed in the X structure; that means it is no longer a half-metallic ferromagnet. The vanishing of the gap was also found for Co_2FeAl in the X structure, but with the Fe atoms aligned ferromagnetically with respect to Co. It is interesting that the $cP16$ structure still exhibits the gap for both pure compounds. From this observation it can be concluded that the existence of the gap is directly related to the occurrence of Co_2 and mixed CrAl(001) planes and that the $L2_1$ structure is not the only possibility for the presence of a HMF gap in Heusler-like compounds X_2YZ.

This finding can be understood easily by considering the symmetry. The magnetization will reduce the symmetry. Applying any special orientation along one of the principal axes (e.g. [001]) will reduce the symmetry from $Fm\bar{3}m$ to $I4/mmm$, at least. This is in accordance with the fact that the O_h point group cannot describe ferromagnetic order. The properties of the electron spin will cause a further reduction to $I4/m$, as vertical mirror operations would change the sign of the spin. In particular, the Γ point of the ferromagnetic Heusler compounds will belong to the $D_{4h}(C_{4h})$ colour group and no longer to O_h, like in the paramagnetic state. The point group in brackets assigns the *magnetic* symmetry with removed vertical mirror planes. The X point becomes Z ($D_{4h}(C_{4h})$) and the point group symmetry of the Λ direction (formerly Δ) is reduced to $C_{4v}(C_4)$ in the ferromagnetic case.

The Γ and Z points of the $cP16$ or $tP4$ structures, as representatives for Cr–Al disorder, have in the ferromagnetic state *also* $D_{4h}(C_{4h})$ symmetry. Therefore, those structures are expected to behave *similarly* to the $L2_1$ structure. However, the local symmetries of the atomic sites in the three structures are different, which may explain the vanishing of the HMF gap in the $tP4$ structure.

The Γ and Z points of the X structure, as representatives for Co–Cr antisite disorder, have in the ferromagnetic state the *lower* $D_{2d}(S_4)$ point group symmetry. Therefore, that structure is expected to behave *differently* from the $L2_1$ structure. Indeed, the most pronounced difference is in the local environment of the atoms in the (001) planes.

The local site symmetries of the atoms are summarized in table 4. It displays the symmetries of atoms and high symmetry points of the Brillouin zone for the different structures for paramagnetic (PM) and ferromagnetic (FM) order. The direction of magnetization was chosen to be along the z axis for FM order. Cr and Al atoms occupy in the $cP16$ structure two inequivalent sites with different local symmetries. The distances between various atoms are given for a fixed lattice parameter a. The X point becomes Z and the Δ direction becomes Λ in tetragonal symmetry. The point group symmetries of the Brillouin zone may serve to avoid confusion about the irreducible representations of bands being different in the PM and FM states.

The Cr magnetic moment is also too small in the mixed $Co_2Cr_{1-x}Fe_xAl$ alloy, as seen from figure 7. The Fe magnetic moment comes close to the value expected from the calculation. This observation points not only on a site disorder but also to a possibility of phase separation resulting in Fe and Cr rich grains of the polycrystalline sample. The overall magnetic moment comes close to the calculated value as a result of the much higher value for Fe compared to Cr. From this observation it is clear that measuring only the total moment is not enough to characterize these alloys completely.

Similar calculations were performed for the half-Heusler compound NiMnSb in order to explain a missing full spin polarization in that compound. In the XYZ $C1_b$ structure one has a series of pure X followed by mixed YZ(001) planes. The calculations were performed for NiMnSb, MnSbNi, and SbNiMn, keeping the lattice parameter fixed. The major difference between the three types is in the local environment of the Ni atoms in the (001) planes. Only in the first type do the alternating (001) planes contain either purely Ni or mixed (MnSb) layers. The exchange of Ni and Mn or Sb resulted in the loss of the HMF character and in turn in a reduction of the spin polarization at the Fermi energy. Indeed, such an intermixing must not prevail through the whole crystal. It is enough just to have disorder in regions close to the surface or interface to explain a reduced spin polarization in spectroscopic methods. These findings are in agreement with the results of Orgassa *et al* [65] for random disorder in NiMnSb.

The assumption of doped, ordered compounds may not hold in every case, especially if one is considering non-half-integer or non-quarter-integer fractions for the iron concentration x. Calculations concerning the spectroscopic properties for more general, non-rational iron concentration, resulting in random alloys, are in preparation. However, the results found here for superstructures are in good agreement to those of Miura *et al* [47] for random alloys.

4. Summary

The electronic structure of the pure and doped Heusler compound $Co_2Cr_{1-x}Fe_xAl$ with varying iron content (x) was calculated by means of different theoretical methods. Element-specific magnetic moments were determined from MCD measurements at the Cr, Fe, and Co $L_{2,3}$ absorption edges of the Heusler alloys Co_2CrAl, $Co_2Cr_{0.6}Fe_{0.4}Al$, and Co_2FeAl.

The calculations revealed a ferromagnetic coupling between the 3d atoms as well as an antiferromagnetic alignment of the Al magnetic moments with respect to the moments of the

3d elements. However, the Al moments are very small and are induced by the surrounding polarized atoms. The calculations predict the $Co_2Cr_{1-x}Fe_xAl$ compound to be a half-metallic ferromagnet. The size of the minority gap ranges from 100 to 800 meV. The smallest band gap around the Fermi edge in the minority bands was found for the compound with $x = 1$. Co_2CrAl and, more pronouncedly, Co_2FeAl turned out to have an indirect Γ–X gap. The mixed compounds exhibit a direct gap at the Γ point, caused by the reduced symmetry.

It was shown that the origin of the minority gap in Co_2CrAl is the geometrical structure and local symmetry of the atoms. It appears in the $L2_1$ structure with successive CrAl and Co_2(001) planes but not in the X structure with successive CoCr and CoAl(001) planes.

In summary, it was shown how theoretical methods can be used to design new materials with predictable magnetic properties.

Acknowledgments

The authors thank all members of NSRRC (Hsinchu, Taiwan) for their help during the beamtime. GHF and SW are very grateful to Yeukuang Hwu (Academia Sinica, Taipei) and his group for support during the experiments in Taiwan.

Financial support by the DFG (FG 559), DAAD (03/314973 and 03/23562), and PROBRAL (167/04) is gratefully acknowledged.

References

[1] Prinz G A 1998 *Science* **282** 1660
[2] de Groot R A, Mueller F M, van Engen P G and Buschow K H J 1983 *Phys. Rev. Lett.* **50** 2024
[3] Coey J M D, Venkatesan M and Bari M A 2002 Half-metallic ferromagnets *Lecture Notes in Physics* vol 595, ed C Berthier, L P Levy and G Martinez (Heidelberg: Springer) pp 377–96
[4] Youn S J and Min B I 1995 *Phys. Rev.* B **51** 10436–42
[5] Ristoiu D, Nozieres J P, Borca C N, Borca B and Dowben P A 2000 *Appl. Phys. Lett.* **76** 2349
[6] Ristoiu D, Nozieres J P, Borca C N, Komesu T, Jeong H-K and Dowben P A 2000 *Eur. Phys. Lett.* **49** 624–30
[7] Zhu W, Sinkovic B, Vescovo E, Tanaka C and Moodera J S 2001 *Phys. Rev.* B **64** R060403
[8] Plogmann S, Schlathölter T, Braun J, Neumann M, Yarmoshenko Y M, Yablonskikh M V, Shreder E I, Kurmaev E Z, Wrona A and Slebarski A 1999 *Phys. Rev.* B **60** 6428
[9] Webster P J and Ziebeck K R A 1973 *J. Phys. Chem. Solids* **34** 1647
[10] Heusler Fr 1903 *Verh. Deutsch. Phys. Ges.* **12** 219
[11] Terada M, Fujita Y and Endo K 1974 *J. Phys. Soc. Japan* **36** 620
[12] Endo K, Ooiwa K and Shinogi A 1992 *J. Magn. Magn. Mater.* **104–107** 2013–4
[13] Ziebeck K R A and Webster P J 1974 *J. Phys. Chem. Solids* **35** 1
[14] van Engen P G, Buschow K H J and Erman M 1983 *J. Magn. Magn. Mater.* **30** 374–82
[15] Yablonskikh M V, Yarmoshenko Y M, Grebennikov V I, Kurmaev E Z, Butorin S M, Duda L-C, Nordgren J, Plogmann S and Neumann M 2001 *Phys. Rev.* B **63** 235117
[16] Ishida S, Akazawa S, Kubo Y and Ishida J 1982 *J. Phys. F: Met. Phys.* **12** 1111–22
[17] Webster P J and Ziebeck K R A 1988 Heusler alloys *Alloys and Compounds of d-Elements with Main Group Elements. Part 2* (*Landolt–Börnstein* Group III *Condensed Matter* vol 19C) (Heidelberg: Springer) pp 104–85
[18] Ziebeck K R A and Neumann K-U 2001 Heusler alloys *Alloys and Compounds of d-Elements with Main Group Elements* part 2 (*Landolt–Börnstein* Group III *Condensed Matter* vol 38C) (Heidelberg: Springer) pp 64–314
[19] Jezierski A 1996 *J. Magn. Magn. Mater.* **164** 381–4
[20] Brown P J, Neumann K-U, Webster P J and Ziebeck K R A 2000 *J. Phys.: Condens. Matter* **12** 1827–35
[21] Yamasaki A, Imada S, Arai R, Utsunomiya H, Suga S, Muro T, Saito Y, Kanomata T and Ishida S 2002 *Phys. Rev.* B **65** 104410
[22] Ishida S, Otsuka Y, Kubo Y and Ishida J 1983 *J. Phys. F: Met. Phys.* **13** 1173–8
[23] Fuji S, Sugimura S, Ishida S and Asano S 1990 *J. Phys.: Condens. Matter* **2** 8583–9
[24] Carbonari A W, Saxena R N Jr, Pendl W, Mestnik Filho J, Attili R N, Olzon-Dionysio M and de Souza S D 1996 *J. Magn. Magn. Mater.* **163** 313–21
[25] Ishida S, Masakai T, Fujii S and Asano S 1998 *Physica* B **245** 1–8
[26] Slebarski A, Jezierski A, Lütkehoff S and Neumann M 1998 *Phys. Rev.* B **57** 6408–12

[27] Picozzi S, Continenza A and Freeman A J 2002 *Phys. Rev.* B **66** 094421
[28] Galanakis I, Dederichs P H and Papanikolaou N 2002 *Phys. Rev.* B **66** 174429
[29] Jezierski A and Borstel G 1995 *Physica* B **205** 397–402
[30] Slebarski A, Jezierski A, Neumann M and Plogmann S 1998 *J. Magn. Magn. Mater.* **185** 43–8
[31] Slebarski A, Talik E, Chelkowska G and Jezierski A 1999 *J. Alloys Compounds* **287** 45–7
[32] Lue C S and Kuo Y-K 2002 *Phys. Rev.* B **66** 085121
[33] Pugaczowa-Michalska M 2003 *Phys. Status Solidi* b **236** 536–9
[34] Block T, Felser C, Jakob G, Ensling J, Mühling B, Gütlich P, Beaumont V, Studer F and Cava R J 2003 *J. Solid State Chem.* **176** 646–51
[35] Felser C, Heitkamp B, Kronast F, Schmitz D, Cramm S, Dürr H A, Elmers H-J, Fecher G H, Wurmehl S, Block T, Valdaitsev D, Nepijko S A, Gloskovskii A, Jakob G, Schönhense G and Eberhardt W 2003 *J. Phys.: Condens. Matter* **15** 7019–27
[36] Kelekar R and Clemens B M 2004 *J. Appl. Phys.* **96** 540
[37] Hirohata A, Kikuchi M, Tezuka N, Inomata K, Claydon J S and Xu Y B 2005 *J. Appl. Phys.* **97** 10C308
[38] Hirohata A, Kurebayashi H, Okamura S, Kikuchi M, Masaki T, Nozaki T, Tezuka N and Inomata K 2005 *J. Appl. Phys.* **97** 103714
[39] Jakob G, Casper F, Beaumont V, Falka S, Auth N, Elmers H-J, Felser C and Adrian H 2005 *J. Magn. Magn. Mater.* **290/291** 1104–7
[40] Inomata K, Okamura S, Goto R and Yezuka N 2003 *Japan. J. Appl. Phys.* **42** L419
[41] Inomata K, Tezuka N, Okamura S, Kurebayashi H and Hirohata A 2004 *J. Appl. Phys.* **95** 7234
[42] Marukame T, Kasahara T, Matsuda K-I, Uemura T and Yamamoto M 2005 *Japan. J. Appl. Phys.* **44** L521–4
[43] Auth N, Jakob G, Block T and Felser C 2003 *Phys. Rev.* B **62** 024403
[44] Conca A, Falk S, Jakob G, Jourdan M and Adrian H 2005 *J. Magn. Magn. Mater.* **290/291** 1127–30
[45] Clifford E, Venkatesan M, Gunning R and Coey J M D 2004 *Solid State Commun.* **131** 61–4
[46] Elmers H-J, Fecher G H, Valdaitsev D, Nepijko S A, Gloskovskii A, Jakob G, Schönhense G, Wurmehl S, Block T, Felser C, Hsu P-C, Tsai W-L and Cramm S 2003 *Phys. Rev.* B **67** 104412
[47] Miura Y, Nagao K and Shirai M 2004 *Phys. Rev.* B **69** 144413
[48] Kobayashi K, Umetsu R Y, Kainuma R, Ishida K, Oyamada T, Fujita A and Fukamichi K 2004 *Appl. Phys. Lett.* **85** 4684
[49] Blaha P, Schwarz K, Sorantin P and Tricky S B 1990 *Comput. Phys. Commun.* **59** 399
[50] Blaha P, Schwarz K, Madsen G K H, Kvasnicka D and Luitz J 2001 *WIEN2k, An Augmented Plane Wave + Local Orbitals Program for Calculating Crystal Properties* Karlheinz Schwarz, Techn. Universitaet Wien, Wien, Austria
[51] Perdew J P, Chevary J A, Vosko S H, Jackson K A, Pederson M R, Singh D J and Fiolhais C 1992 *Phys. Rev.* B **46** 6671
[52] Savrasov S Y 1996 *Phys. Rev.* B **54** 16470
[53] Tobola J, Pierre J, Kaprzyk S, Skolozdra R V and Kouacou M A 1996 *J. Magn. Magn. Mater.* **159** 192–200
[54] de Groot R A, Mueller F M, van Engen P G and Buschow K H J 1984 *J. Appl. Phys.* **55** 2151
[55] Öğüt S and Rabe K M 1995 *Phys. Rev.* B **51** 10443–53
[56] Skomski R and Dowben P A 2002 *Europhys. Lett.* **58** 544–8
[57] Dowben P A and Skomski R 2003 *J. Appl. Phys.* **93** 7948
[58] Chioncel L, Katsnelson M I, de Groot R A and Lichtenstein A I 2003 *Phys. Rev.* B **68** 144425
[59] Buschow K H J and van Engen P G 1981 *J. Magn. Magn. Mater.* **25** 90–6
[60] Slebarski A, Neumann M and Schneider B 2001 *J. Phys.: Condens. Matter* **13** 5515–8
[61] Kellou A, Fenineche N E, Grosdidier T, Aourag H and Coddet C 2003 *J. Appl. Phys.* **94** 3292
[62] Lin W and Freeman A J 1992 *Phys. Rev.* B **45** 61
[63] Bacon G E and Plant J S 1971 *J. Phys. F: Met. Phys.* **1** 524–32
[64] Feng Y, Rhee J Y, Wiener T A, Lynch D W, Hubbard B E, Sievers A J, Schlagel D L, Lograsso T A and Miller L L 2001 *Phys. Rev.* B **63** 165109
[65] Orgassa D, Fujiwara H, Schulthess T C and Butler W H 1999 *Phys. Rev.* B **60** 13237